

# NaturalGAIA: Pushing the Frontiers of GUI Agents with a Challenging Benchmark and High-Quality Trajectory Dataset

Zihan Zheng<sup>1\*</sup>, Tianle Cui<sup>1\*</sup>, Chuwen Xie<sup>1</sup>, Jiahui Zhang<sup>1</sup>, Jiahui Pan<sup>1</sup>, Lewei He<sup>1†</sup> Qianglong Chen<sup>2†</sup>,

<sup>1</sup>South China Normal University

<sup>2</sup>Zhejiang University

zhengzihan994@m.scnu.edu.cn, helewei@m.scnu.edu.cn, chenqianglong@zju.edu.cn

## Abstract

The rapid advancement of Large Language Model (LLM)-driven Graphical User Interface (GUI) agents is significantly hampered by the profound limitations of existing evaluation benchmarks in terms of accuracy, reproducibility, and scalability. To address this critical gap, we introduce NaturalGAIA, a novel benchmark engineered on the principle of Causal Pathways. This design paradigm structures complex tasks into a series of programmatically verifiable atomic steps, ensuring a rigorous, fully automated, and reproducible standard for assessment. Concurrently, to mitigate the inherent capability deficits of agents, we developed LightManus, a hierarchical agent architecture specifically optimized for long-horizon tasks. We leveraged this agent to generate a high-quality, human-verified trajectory dataset that uniquely captures diverse and even self-correcting interaction patterns of LLMs. We then utilized this dataset to perform Reinforcement Fine-Tuning (RFT) on the Qwen2.5-VL-7B model. Our experiments reveal that NaturalGAIA presents a formidable challenge to current state-of-the-art LLMs; even the top-performing Claude-sonnet-4 achieved a Weighted Pathway Success Rate (WPSR) of only 34.6%. Moreover, while RFT substantially improved the smaller model’s GUI execution capabilities (WPSR increased from 3.3% to 10.8%), its performance degraded sharply when handling complex scenarios. This outcome highlights the inherent capability ceiling of smaller models when faced with comprehensive tasks that integrate perception, decision-making, and execution. This research contributes a rigorous evaluation standard and a high-quality dataset to the community, aiming to guide the future development of GUI agents.

## 1 Introduction

The emergence of LLM-driven GUI agents (DeepSeek-AI et al. 2025; OpenAI et al. 2024b; Qwen et al. 2025) represents a significant advance over traditional automation (Yang et al. 2023; Zhang et al. 2023; Tang et al. 2025; Liu et al. 2025a; Durante et al. 2024), yet their progress is difficult to assess due to severe limitations in existing benchmarks. Current evaluation methods often rely on ambiguous final-state verification, which depends on fallible MLLMs (Bai et al. 2023; OpenAI et al. 2024a) and costly manual checks, thus compromising the scalability, reproducibility,

and automation of evaluations (Mialon et al. 2023; Rawles et al. 2024). Moreover, these benchmarks inadequately measure performance on long-horizon tasks and fail to consider diverse valid solution paths, resulting in insufficient evaluation comprehensiveness (Liu et al. 2023; Li et al. 2025a; Chezelles et al. 2025).

Concurrently, these agents exhibit significant deficits in handling complex, real-world workflows, a problem exacerbated by prevailing learning paradigms (Koh et al. 2024b; Xu et al. 2024). Agents trained on successful execution traces (Wang et al. 2025; Jiang et al. 2025; Qiu et al. 2025) tend to form rigid “shortcut” strategies. While effective for repeated tasks in static environments, this approach leads to poor generalization and robustness in novel scenarios, indicating a reliance on memory over transferable knowledge (Cheng et al. 2024; He et al. 2024; Gou et al. 2025). These generalization failures fundamentally stem from the LLM’s deficiencies in GUI operational knowledge and long-range planning (Ye et al. 2025b; Muennighoff et al. 2025; Huang et al. 2024), a constraint rooted in the scarcity of high-quality, structured trajectory data (He, Jin, and Liu 2025).

To address these issues, we introduce NaturalGAIA, a novel benchmark with 276 tasks designed to address critical evaluation challenges in GUI agents. Unlike benchmarks such as GAIA(Mialon et al. 2023) that focus on flexible, goal-oriented reasoning, NaturalGAIA is engineered to rigorously test an agent’s ability to execute complex, structured procedures reliably. This is achieved through Causal Pathways (CPs)—task structures that model realistic, high-frequency user workflows across multiple platforms, thereby simulating how humans sequentially use tools to achieve goals. Each pathway is composed of interdependent, programmatically verifiable atomic steps. An error at any step triggers a deterministic “Path Collapse”, which not only provides an unambiguous failure signal but also pinpoints the source of the failure. Consequently, NaturalGAIA ensures task complexity and generalizability while significantly enhancing evaluation timeliness, accuracy, and automation, thereby establishing a rigorous and reproducible standard for assessing GUI agents.

Furthermore, advanced learning paradigms were explored to advance the capabilities of GUI agents. We developed a hierarchical agent architecture featuring a Task Parser and a Workflow Manager to improve long-horizon task handling

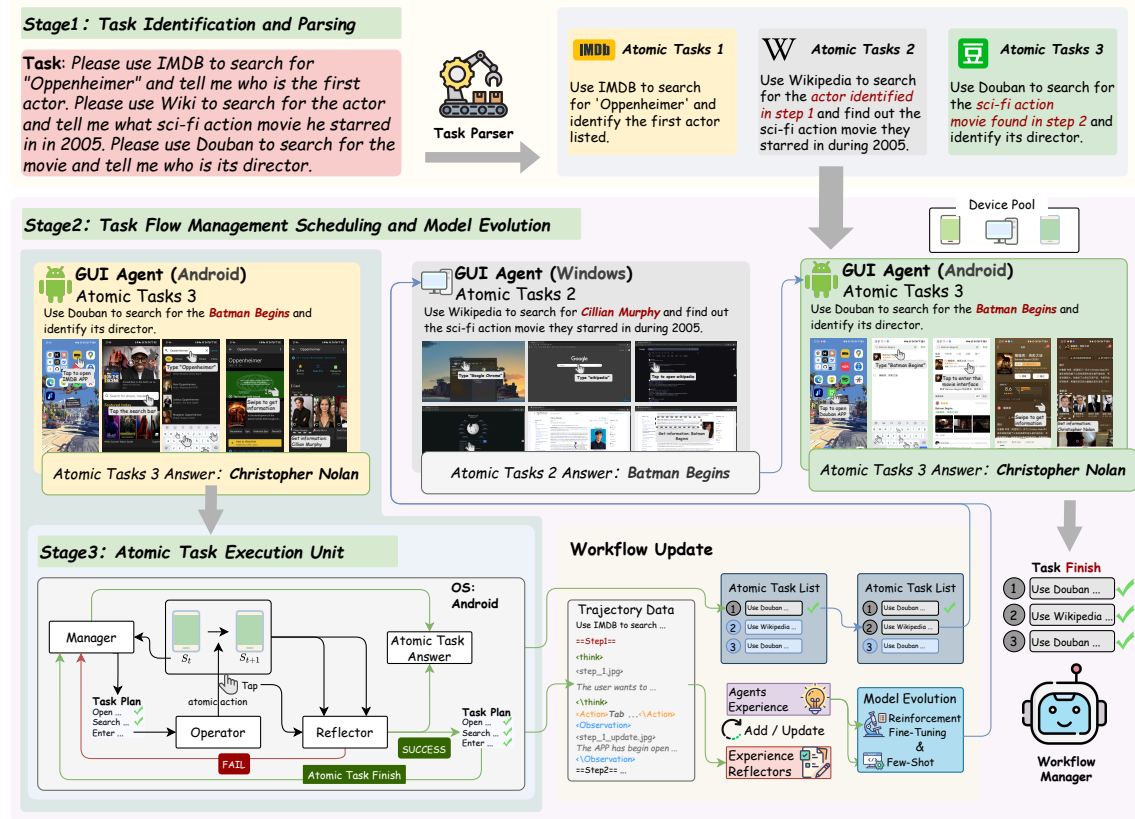


Figure 1: An overview of our three-stage framework **LightManus**, executing a complex, cross-platform task from Natural-GAIA. **Task Parsing** (Stage 1): A complex instruction is decomposed into a sequence of atomic tasks that form a Causal Pathway. **Workflow Management & Evolution** (Stage 2): The system schedules these tasks across different devices and uses collected Trajectory Data for model evolution via RFT. **Atomic Task Execution Unit** (Stage 3): This core unit, comprising a Manager, Operator, and Reflector, handles the execution of each atomic task.

through effective decomposition and dynamic scheduling. Additionally, we constructed a high-quality GUI operation trajectory dataset. Generated by our agent and iteratively refined through expert validation, this dataset ultimately contains 523 trajectories with detailed planning rationale. It was subsequently used to investigate the efficacy of Reinforcement Fine-Tuning (RFT) and serves as a foundational resource for developing next-generation agents. A representative example is presented in Figure 1.

Experimental results demonstrate that our hierarchical agent, LightManus (driven by Claude-sonnet-4), significantly outperforms mainstream baselines with a 42.9% Pass@1 success rate, yet achieves only a 34.6% Weighted Pathway Success Rate (WPSR) on our NaturalGAIA. We also validated the efficacy of our collected data through RFT, which substantially enhanced the Qwen2.5-VL-7B model’s capability by increasing its WPSR from 3.3% to 10.8%. However, this enhancement does not generalize to complex, long-horizon tasks where performance degrades sharply. These findings reveal a critical gap between specialized, data-driven skill acquisition and the generalizable, long-range planning required for true GUI autonomy.

The main contributions of this paper can be summarized as follows:

- We introduce NaturalGAIA, a novel benchmark meticulously designed around Causal Pathways principles and equipped with a multi-level evaluation framework to precisely evaluate agent performance on complex, long-horizon tasks. Experimental results reveal that even state-of-the-art models encounter a formidable challenge on this suite.
- We construct and publicly release a high-quality dataset of GUI operation trajectories, comprising 523 trajectories curated through an iterative process of LLM generation and rigorous human verification, to provide a critical resource for future agent training.
- We conduct an in-depth investigation into trajectory-based reinforcement fine-tuning. This study offers initial evidence and key insights into leveraging this method efficiently to enhance agent capabilities.

## 2 Related Work

The advancement of GUI agents faces three principal challenges. First, an evaluation-realism dilemma persists in

benchmarks. While environments have evolved towards higher fidelity, from web-based (Zhou et al. 2023; Koh et al. 2024a) to mobile-centric (Chai et al. 2025) and long-horizon tasks (Ye et al. 2025a), this pursuit of realism compromises scientific rigor. The dynamic nature of modern applications impedes reproducibility (Garg et al. 2025), and the existence of multiple valid solution paths renders fixed trajectory matching unreliable (Zhou et al. 2023; Liu et al. 2023), often necessitating costly or fallible evaluations (Chai et al. 2025; Mialon et al. 2023). Second, a data bottleneck constrains the development of increasingly sophisticated agents. Advances in high-resolution visual perception (Hong et al. 2024; Li et al. 2025b; Cheng et al. 2024) and modular architectures (Zhang et al. 2025, 2024; Wang et al. 2024) demand structured, fine-grained data that existing datasets lack. Third, a deficit of experiential data hinders the shift from simple imitation learning (Rasheed et al. 2024; Deng et al. 2023) to more advanced paradigms like learning from self-exploration (Wang et al. 2023; Jiang et al. 2025) or trial-and-error (Shinn et al. 2023; Qiu et al. 2025; Wang et al. 2024), which require diverse trajectory data. This work addresses these gaps directly.

NaturalGAIA resolves the evaluation dilemma by providing a stable, reproducible, and fully automated benchmark with programmatically verifiable answers. Concurrently, our trajectory dataset addresses both the data bottleneck and the experiential data deficit by supplying structured and diverse interaction data to foster the development of more capable and robust agents.

### 3 NaturalGAIA

While prominent benchmarks such as GAIA excel at assessing flexible, goal-oriented reasoning, they lack rigorous testing of an agent’s ability to reliably execute complex, structured procedures grounded in natural user tasks. To fill this gap, NaturalGAIA introduces Causal Pathways (CPs)—a task architecture of strict, causally-dependent sequences explicitly designed to model these authentic, cross-platform procedures. In this framework, any procedural error triggers a deterministic Path Collapse, yielding an unambiguous, process-level failure signal that transcends the limitations of final-state evaluations. NaturalGAIA thus functions as a precise diagnostic tool, designed to probe an agent’s core capabilities in long-range planning, memory, and operational fidelity.

#### 3.1 Atomic Tasks: The Fundamental Nodes of Causal Pathways

At the core of NaturalGAIA are *atomic tasks*—the smallest indivisible units of interaction. Each atomic task is designed to retrieve a single, specific piece of information (i.e., the “answer”) through a sequence of primitive GUI operations. Importantly, every atomic task is associated with a unique and deterministic correct answer, allowing for objective, automated evaluation. This granularity enables the benchmark to assess an agent’s performance in perception, interface manipulation, and reasoning independently. By isolating each task’s input, action sequence, and output, NaturalGAIA fa-

cilitates precise error analysis and supports targeted improvements in sub-capabilities. These atomic tasks serve as the fundamental nodes that constitute each Causal Pathway.

#### 3.2 Causal Pathways: Structuring Tasks with Logical Dependencies

The core construct of NaturalGAIA is the Causal Pathway (CP), an executable representation of procedural knowledge for structured tasks. A key design principle is the decoupling of a CP’s abstract logic from its physical execution across diverse platforms, such as different applications or websites. This allows for the flexible generation of varied task instances to mitigate data contamination and model overfitting, while simultaneously upholding the rigorous evaluation of underlying causal dependencies.

Nodes within a CP are linked by strict causal dependencies, where an error at any step triggers a “Path Collapse”—a deterministic failure of the entire sequence. This mechanism provides an unambiguous signal, pinpointing the exact moment an agent’s execution deviates from the required causal logic. Consequently, NaturalGAIA evaluates not just task completion but, more critically, an agent’s capacity for long-range planning, abstract reasoning, and robust execution.

The specific construction principles and processes of CPs and tasks in NaturalGAIA are shown in Appendix A1 and A2 respectively.

#### 3.3 Multi-level Evaluation Framework

To precisely evaluate agent performance within NaturalGAIA and meticulously identify the root causes of errors, this study constructs a hierarchical evaluation framework. This framework enables comprehensive scrutiny from macroscopic, difficulty-weighted task completion down to microscopic error attribution.

**Level 1: Weighted Pathway Success Rate (WPSR)** To account for task complexity, we introduce a difficulty score  $D_{j,i}$  for each task instance  $i$  of a Causal Pathway  $CP_j$ . This score is proportional to the number of nodes in the pathway and the number of distinct applications involved in its corresponding task. WPSR is defined by weighting each successful completion ( $\mathbb{S}_{\text{task}}(j, i) = 1$ ) by its normalized difficulty  $w_{j,i} = D_{j,i} / \sum_{k,l} D_{k,l}$ , where the sum in the denominator is over all task instances across all pathways.

$$\text{WPSR} = \sum_{j,i} w_{j,i} \cdot \mathbb{S}_{\text{task}}(j, i)$$

WPSR serves as a holistic metric for an agent’s final task completion capability, weighted by difficulty.

**Level 2: Fine-grained Traversal Metrics** To quantify partial progress and resilience, we introduce two complementary metrics that assess traversal quality.

**Mean Atomic Tasks Completion Ratio (MATCR):** This metric quantifies an agent’s ability to successfully complete sequences of atomic tasks. For each task sequence  $j$  within the benchmark, a completion ratio  $R_j = k_j/n_j$  is calculated, where  $k_j$  is the number of consecutive atomic tasks

successfully executed from the start, and  $n_j$  is the total number of atomic tasks in sequence  $j$ .

$$\text{MATCR} = \frac{1}{N} \sum_{j=1}^N \frac{k_j}{n_j}$$

**Positional-Weighted Atomic Tasks Success Rate (p-ATSR):** This metric evaluates an agent’s ability to maintain long-term coherence by assigning greater weight to successes in the later stages of a Causal Pathway. Let  $n_j$  be the total number of atomic tasks in pathway  $CP_j$ . We introduce a positional weight, denoted as  $p(i)$ , which is a monotonically increasing function of the step index  $i$ . The p-ATSR is then defined as:

$$\text{p-ATSR} = \frac{\sum_{j=1}^N \sum_{i=1}^{n_j} p(i) \cdot \mathbb{S}_{\text{atomic}}(j, i)}{\sum_{j=1}^N \sum_{i=1}^{n_j} p(i)}$$

where  $\mathbb{S}_{\text{atomic}}(j, i) = 1$  for a success at step  $i$  of pathway  $j$ , and 0 otherwise.

In summary, MATCR assesses an agent’s foundational reliability by quantifying its average execution length, whereas p-ATSR places greater emphasis on its long-term coherence by rewarding success in the later stages of a task.

**Level 3: Error Attribution Analysis** For atomic tasks that fail, as identified by the Level 2 metrics, this stage involves analyzing the atomic operation sequence to attribute Execution Errors (EE) to one of three primary types:

- *Knowledge Deficit (KD)*: The agent lacks the necessary domain-specific or procedural knowledge regarding application operations or function invocation required to achieve the objective.
- *Perceptual Error (PE)*: Although the agent possesses the correct intent and planning, it fails during the information extraction phase due to misreading or misinterpretation of visual or textual information from the interface.
- *Operational Error (OE)*: The agent understands the task and correctly perceives the interface, but fails to take appropriate or precise actions during specific operations.

### 3.4 Task Difficulty Stratification

To enable a systematic evaluation of agent capabilities, tasks in NaturalGAIA are stratified into three difficulty levels. This stratification is defined by the structural properties of their underlying Causal Pathways, including their length (number of nodes), the complexity of transitions between nodes, and the diversity of applications involved.

**Level 1:** Consisting of short Causal Pathways involving 1-2 atomic tasks (nodes). These tasks typically operate within 1-2 applications and assess an agent’s basic sequential execution and information-passing capabilities.

**Level 2:** Featuring Causal Pathways of intermediate length, containing 3-4 nodes. These pathways often require transitions across 3-5 different applications or involve complex interactions within a smaller set of applications, testing an agent’s ability to maintain context over a longer duration.

**Level 3:** Involving complex and lengthy Causal Pathways spanning 5-7 nodes and 3-7 applications. Successfully traversing these pathways demands advanced planning, long-term memory, and robust handling of intricate inter-node dependencies, posing a significant challenge to the agent’s cognitive and operational architecture.

Finally, we constructed 276 tasks. Data statistics and examples of tasks at different levels are shown in the Appendix A3 and A4.

## 4 Method

### 4.1 Cross-Platform Agent Architecture

To facilitate the generation of high-quality, long-horizon task trajectories, this study introduces LightManus, a specialized framework engineered for complex, cross-platform operations. Its hierarchical architecture is systematically organized into three distinct stages. The first stage, Task Parsing, analyzes the high-level user instruction and decomposes it into a logical sequence of executable sub-tasks. The second stage, the Workflow Manager, orchestrates this sequence by dynamically scheduling and delegating each sub-task to the appropriate device. The final stage is the Atomic Task Execution Unit, which executes the ground-level operations. This unit consists of specialized low-level agents—Mobile-Agent-e (Wang et al. 2025) for Android and PC-Agent (Liu et al. 2025b) for PC—that handle direct interaction with the graphical user interface. This structured, three-stage design provides a robust mechanism for generating high-fidelity execution trajectories and optimizes long-horizon task performance by ensuring seamless coordination across disparate operating systems.

### 4.2 Human-Verified Trajectory Collection

To construct a high-quality dataset aimed at enhancing the capabilities of GUI agents, we implemented a **rigorous** two-phase data collection pipeline. This methodology is designed to synergize the scalability and diverse exploratory power of a Large Language Model (LLM)-driven agent with the precision and reliability of human experts. The core motivation is to create a dataset that not only ensures procedural correctness but also captures a rich diversity of interaction behaviors, thereby transcending the traditional paradigm of singular, “optimal” paths.

**Phase 1: LLM-Driven Trajectory Generation** The data generation process was initiated using 265 unique atomic tasks as prompts. Our agent, LightManus, powered by Gemini-2.5-Pro, was tasked with autonomously completing these tasks. For each task, LightManus engaged in a **cyclical action process** at every step, which can be decomposed as follows:

- **Perception and State Understanding:** The agent first captures and analyzes the current user interface (UI) screenshot.
- **Deliberation and Planning:** The agent integrates the task objective with visual information to perform multi-level reasoning. This includes a high-level Thought process to maintain the overall plan and a micro-level

Action Thought to determine the specific UI operation to be executed.

- **Action Execution:** The agent formulates and dispatches the determined action command.
- **Observation and Reflection:** Following the action, the agent captures and observes the new interface state, then provides feedback on the outcome to reflect on its progress toward the goal.

This automated procedure yielded an initial corpus of over 600 successfully executed trajectories. However, this raw corpus suffered from a critical flaw that necessitated curation: in certain instances, the model would bypass genuine UI interaction by directly generating answers from its internal, parametric knowledge. This highlighted the indispensable value of the human verification phase.

**Phase 2: Expert Verification and Curation** Every successfully generated trajectory was subjected to a meticulous review by a team of two graduate researchers. This review involved a detailed source-trace analysis of all execution information, including step-by-step screenshots and corresponding log files. Through an iterative refinement of this analysis, 523 trajectories were ultimately curated for the final dataset, adhering to the following principles:

- **Enforcing Grounded Execution:** A trajectory was deemed valid only if all of the agent’s actions were strictly grounded in the visual information presented on-screen. This principle explicitly filters out any solutions derived from the model’s internal knowledge, ensuring the data reflects genuine agent-environment interaction.
- **Preserving Behavioral Diversity and Corrective Processes:** Our curation criteria deliberately deviate from selecting only the “most efficient” paths, aiming instead to retain a variety of valid interaction strategies. Furthermore, we intentionally preserved trajectories containing recoverable *error steps*—cases where the agent successfully self-corrects through reflection after executing an erroneous action or exploring a wrong path. We posit that these trajectories, containing corrective processes, provide an invaluable learning signal for training more robust agents capable of reasoning about and recovering from their own errors.

### 4.3 Final Data Structure

The curated dataset is composed of structured data points, each containing the initial instruction, the final solution, and the interaction trajectory. A complete trajectory  $T$  is represented as a sequence of time steps,  $T = (t_1, t_2, \dots, t_n)$ . Each time step  $t_i$  is defined as a tuple  $(s_i, R_i, a_i, s_{i+1}, o_i)$  that encapsulates a full state transition, where:  $s_i$  is the initial state before the action, represented by a UI screenshot.  $R_i$  is the agent’s cognitive reasoning trace, encapsulating its high-level strategic Thought and micro-level Action Thought.  $a_i$  is the specific Action executed by the agent in that step.  $s_{i+1}$  is the new state reached after executing action  $a_i$ , also represented by a UI screenshot.  $o_i$  is the agent’s Observation and reflection on the outcome of the state transition from  $s_i$  to  $s_{i+1}$ .

This granular, structured format transparently captures the agent’s complete perception-reasoning-action loop, making it an ideal resource for process-supervision and model fine-tuning. We present detailed trajectory data samples and corresponding visualization execution trajectories in the Appendix B.

### 4.4 Trajectory-based LLM Enhancement

The enhancement of the Qwen-2.5-VL-7B model was conducted via Trajectory-Reinforced Fine-Tuning (T-RFT), a methodological choice deliberately positioned between two common paradigms: Supervised Fine-Tuning (SFT) and end-to-end Reinforcement Learning (RL). While SFT offers a straightforward approach by mimicking expert demonstrations, it typically yields brittle policies that overfit to the specific, static trajectories seen during training. This reliance on behavioral cloning limits the agent’s ability to generalize to novel situations or recover from errors. Conversely, conventional end-to-end RL, though theoretically more robust, is often practically infeasible for complex GUI tasks. It necessitates extensive online exploration, entailing prohibitive computational overhead, significant communication latency, and long training durations.

T-RFT presents a pragmatic and resource-efficient alternative. By leveraging a high-quality, static dataset of human-verified trajectories, it circumvents the need for costly online interaction. Yet, unlike SFT, it moves beyond simple imitation by applying policy optimization principles to learn a more generalizable decision-making model. This allows the agent to distill robust navigational strategies from the expert data, rather than merely memorizing action sequences. Ultimately, this approach was chosen to specifically augment the model’s capacity to interpret and strategically act upon the sequential visual and textual inputs inherent to GUI environments.

## 5 Experiment

### 5.1 Setup

**Baselines.** The performance of our proposed Light-Manus framework was benchmarked against two baseline agents: PC-Agent (PCA) for desktop environments and Mobile-Agent-e (MAe) for Android environments.

**Foundation Models.** Our evaluation includes a diverse range of state-of-the-art proprietary and open-source MLLMs. Proprietary models include Google’s Gemini series (Gemini-2.5-Pro, Gemini-2.5-Flash), OpenAI’s GPT-03, and Anthropic’s Claude-sonnet-4. Open-source models assessed are from the Qwen series, including Qwen3-235B-A22B, Qwen2.5-Max, and the base Qwen2.5-VL-7B model which was targeted for fine-tuning.

**Training.** The enhancement of the smaller model was achieved through T-RFT. Specifically, the Qwen2.5-VL-7B model was fine-tuned using our curated dataset comprising 278 human-verified trajectories. The training was executed on a high-performance computing cluster equipped with four NVIDIA A100 GPUs. Further training details can be found in Appendix C.

| Method                | Level-1     |              |             |             |             |             | Level-2     |             |             |             |             |             | Level-3     |             |             |             |             |             | Overall     |             |  |  |
|-----------------------|-------------|--------------|-------------|-------------|-------------|-------------|-------------|-------------|-------------|-------------|-------------|-------------|-------------|-------------|-------------|-------------|-------------|-------------|-------------|-------------|--|--|
|                       | SR          |              | WPSR        | MATCR       | pATSR       | SR          |             | WPSR        | MATCR       | pATSR       | SR          |             | WPSR        | MATCR       | pATSR       | SR          |             | WPSR        | MATCR       | pATSR       |  |  |
|                       | P@1         | P@4          |             |             |             | P@1         | P@4         |             |             |             | P@1         | P@4         |             |             |             | P@1         | P@4         |             |             |             |  |  |
| <b>PC-Agent</b>       |             |              |             |             |             |             |             |             |             |             |             |             |             |             |             |             |             |             |             |             |  |  |
| • Gemini-2.5-Pro      | 40.0        | 66.7         | 37.5        | 60.7        | 54.1        | 10.0        | 40.0        | 12.5        | 43.1        | 31.8        | 0.0         | 20.0        | 5.1         | 25.0        | 16.0        | 20.0        | 45.7        | 14.6        | 38.6        | 25.8        |  |  |
| <b>Mobile-Agent-e</b> |             |              |             |             |             |             |             |             |             |             |             |             |             |             |             |             |             |             |             |             |  |  |
| • Gemini-2.5-Pro      | 46.7        | <b>100.0</b> | 57.1        | <b>75.0</b> | 70.0        | 10.0        | <b>60.0</b> | 20.0        | 52.5        | 41.9        | 0.0         | <b>30.0</b> | 9.3         | 24.6        | 17.2        | 22.9        | <b>68.6</b> | 23.2        | 44.5        | 31.6        |  |  |
| <b>LightManus</b>     |             |              |             |             |             |             |             |             |             |             |             |             |             |             |             |             |             |             |             |             |  |  |
| • Gemini-2.5-Pro      | <b>73.3</b> | <b>100.0</b> | <b>60.7</b> | 71.4        | <b>72.7</b> | 20.0        | <b>70.0</b> | 27.5        | <b>53.1</b> | 46.4        | <b>10.0</b> | <b>40.0</b> | <b>16.9</b> | 29.7        | <b>23.9</b> | <b>40.0</b> | <b>74.3</b> | <b>29.9</b> | 46.3        | <b>37.1</b> |  |  |
| • Gemini-2.5-Flash    | 53.3        | <u>93.3</u>  | <b>62.5</b> | <u>74.1</u> | <u>70.7</u> | 0.0         | <u>60.0</u> | 22.5        | 50.0        | 42.7        | 0.0         | <u>30.0</u> | <u>11.4</u> | 20.3        | <u>15.7</u> | <u>22.9</u> | <u>65.7</u> | 26.2        | 41.5        | <u>31.1</u> |  |  |
| • GPT-o3              | <u>60.0</u> | -            | 57.1        | 67.9        | <u>64.5</u> | <u>30.0</u> | -           | <u>30.0</u> | <b>57.5</b> | <u>49.6</u> | 0.0         | -           | 0.0         | <u>32.2</u> | 20.8        | <u>34.3</u> | -           | 22.0        | <u>48.0</u> | 35.1        |  |  |
| • Claude-sonnet-4     | <u>60.0</u> | -            | 57.1        | 60.7        | 59.1        | <b>40.0</b> | -           | <b>40.0</b> | <b>57.5</b> | <b>52.1</b> | <b>20.0</b> | -           | <b>20.3</b> | <b>37.3</b> | <b>30.0</b> | <b>42.9</b> | -           | <b>34.6</b> | <b>48.8</b> | <b>40.4</b> |  |  |
| • Qwen3               | 40.0        | 60.0         | 28.6        | 50.0        | 44.5        | 0.0         | 30.0        | 10.0        | 32.5        | 25.2        | <u>10.0</u> | 10.0        | 5.1         | 16.1        | 10.2        | 20.0        | 37.1        | 11.8        | 28.7        | 19.2        |  |  |
| • Qwen2.5-Max         | <u>60.0</u> | <u>86.7</u>  | 50.0        | <u>58.9</u> | <u>55.9</u> | 10.0        | 20.0        | 10.0        | 30.6        | 23.2        | <u>10.0</u> | 20.0        | 4.7         | 11.0        | 7.5         | <u>31.4</u> | <u>48.6</u> | 16.3        | 27.8        | 18.6        |  |  |
| • Qwen2.5-7B          | 6.7         | 26.7         | 7.1         | 18.8        | 15.7        | 10.0        | 10.0        | 2.5         | 21.9        | 15.1        | 0.0         | 10.0        | 2.1         | 14.8        | 7.8         | 5.7         | 17.1        | 3.3         | 17.9        | 11.0        |  |  |
| • Qwen2.5-7B-RFT      | 33.3        | 73.3         | 28.6        | 40.2        | 37.0        | 10.0        | 20.0        | 7.5         | 23.8        | 17.3        | 0.0         | 20.0        | 4.7         | 16.5        | 10.0        | 17.1        | 42.8        | 10.8        | 24.0        | 15.8        |  |  |

Table 1: Main results on the NaturalGAIA, comparing the performance of different agent frameworks and foundation models across varying task difficulty levels. We evaluate using Success Rate (SR%) at Pass@1 and Pass@4, Weighted Pathway Success Rate (WPSR%), Mean Atomic Tasks Completion Ratio (MATCR%), and Positional-Weighted Atomic Tasks Success Rate (p-ATSR%). Our proposed LightManus framework consistently outperforms baseline agents. While Reinforcement Fine-Tuning (RFT) remarkably improves the smaller model’s performance, its effectiveness diminishes as task complexity increases.

## 5.2 Main Results

The experimental results, detailed in Table 1, reveal several key findings. Our proposed LightManus framework consistently demonstrates superior performance over baseline agents across all evaluated metrics. Among the foundation models, large-scale proprietary models, particularly Claude-sonnet-4 and Gemini-2.5-Pro, exhibit the most robust capabilities, achieving the highest success rates on complex, long-horizon tasks. While open-source models show promise, a discernible performance gap remains. Furthermore, T-RFT substantially enhances the capabilities of smaller models on basic tasks, yet this advantage diminishes markedly with increasing task complexity, highlighting the intrinsic limitations of model scale. The subsequent analysis dissects these findings by evaluating the distinct contributions of the agent framework, the foundation models, and the fine-tuning process.

**Framework Efficacy: The Architectural Advantage of LightManus** The LightManus framework demonstrates a significant advantage in GUI execution tasks. Driven by the same Gemini-2.5-Pro model, LightManus’s overall performance surpasses that of PCA and MAe. Specifically, its success rate (Pass@1) reaches 40.0%, which is considerably higher than PCA’s 20.0% and MAe’s 22.9%. Its WPSR is 29.9%, also outperforming PCA’s 14.6% and MAe’s 23.2%.

This superior performance stems from its higher execution reliability and long-horizon coherence. LightManus, powered by Gemini-2.5-Pro, shows substantial leads in both MATCR (46.3% vs. 39.2%/43.1%) and p-ATSR (37.1% vs. 25.8%/31.6%) metrics. A particularly compelling piece of evidence is that LightManus equipped with the smaller Gemini-2.5-Flash achieves a p-ATSR (31.1%) that is comparable to that of MAe equipped with the more powerful Gemini-2.5-Pro (31.6%). This result strongly indicates that the framework design of LightManus provides more robust execution support for complex, long-horizon tasks.

**The Impact of LLM Scale on Performance** The experimental results clearly reveal the critical impact of LLM scale on performance. Larger models, with their extensive knowledge bases, yield higher operational reliability. This is reflected in the MATCR metric: LightManus driven by Gemini-2.5-Pro (46.3%) outperforms its Gemini-2.5-Flash version (41.5%), indicating that larger models can execute atomic operations more stably.

However, a counter-intuitive phenomenon was observed in simple tasks: larger models occasionally exhibit a tendency to “over-plan”, breaking down simple instructions into excessively verbose steps. For instance, in Level-1 tasks, the agent equipped with Gemini-2.5-Flash slightly outperformed in WPSR (62.5% vs. 60.7%) and MATCR (74.1% vs. 71.4%). This suggests that for low-complexity tasks, the more concise planning strategy of smaller models can sometimes be more efficient.

**Efficacy and Limitations of Small Model Specialization** Fine-tuning smaller models highlights both their potential and inherent limitations. By fine-tuning Qwen2.5-VL-7B with our trajectory data, the model’s performance on basic tasks was significantly enhanced. In Level-1 tasks, its Pass@1 success rate increased nearly fivefold (6.7% → 33.3%), WPSR nearly quadrupled (7.1% → 28.6%), and MATCR also doubled (18.8% → 40.2%).

However, this specialized capability gained through fine-tuning does not generalize well to complex scenarios. As task complexity increases, the model’s intrinsic capability ceiling becomes apparent. Its WPSR plummets from 28.6% at Level-1 to 7.5% at Level-2 and 4.7% at Level-3. This precipitous decline in performance indicates that core capabilities required for executing complex GUI tasks, such as long-range planning and memory, cannot be compensated for solely by fine-tuning on domain-specific data.

| Model             | SR(%) |
|-------------------|-------|
| Qwen2.5-VL-7B     | 26.3  |
| Qwen2.5-VL-7B-RFT | 36.8  |

Table 2: Generalization performance on the A3 benchmark (Chai et al. 2025). The evaluation is conducted on applications unseen during training to assess the model’s transferability.

### 5.3 Generalization Across Application Scenarios

As shown in table 2, to rigorously evaluate the model’s ability to generalize to new environments, we conducted a supplementary experiment on the A3 benchmark (Chai et al. 2025). For this test, we selected six task subsets involving applications that are entirely disjoint from those present in our training trajectory data. This setup ensures a stringent assessment of transferable skills rather than memorized procedures. The results show that the base Qwen2.5-VL-7B model achieved a success rate of 26.3%. After T-RFT, the model’s performance on these novel applications rose to 36.8%, representing a substantial relative improvement of approximately 40%. This marked enhancement strongly suggests that the fine-tuning process did not lead to overfitting. Instead, it indicates the model has internalized more generalizable operational principles for GUI interaction, underscoring the value of our high-quality trajectory data in fostering robust and transferable agent capabilities.

### 5.4 Error analysis

As shown in Figure 2, we classify agent failures into three primary types: Planning & Reasoning Errors (PRE), which refer to when the agent formulates a logically flawed sequence of steps; Structural Compliance Errors (SCE), where the model fails to generate output in the required action format; and Execution Errors (EE), a category that encompasses the finer-grained Operational Errors (OE), Knowledge Deficits (KD), and Perceptual Errors (PE).

The error analysis reveals significant disparities in failure modes among the models. High-performance models, such as the Gemini series (-2.5-Pro and -2.5-Flash), exhibits low PRE and SCE rates, demonstrating robust capabilities in planning and structural compliance. Their failures are predominantly concentrated in EE, accounting for 47.8% and 54.3% of their respective outcomes. A deeper analysis of the EE category shows that the primary bottleneck for Gemini-2.5-Pro is OE (35.7%), highlighting a challenge in execution accuracy. For the smaller Gemini-2.5-Flash, its EE composition is more heavily skewed towards KD (19.3% vs. 5.0%), reflecting a trade-off between model scale and embedded knowledge.

In contrast, the Qwen2.5-VL-7B series of models exhibits a more fundamental bottleneck. The root cause of failure for the base model is a critical rate of SCE (46.4%), followed by EE (42.2%). While T-RFT substantially reduces the total EE rate from 42.2% to 30.0%, this improvement is almost entirely attributable to the successful mitigation of KD (32.9% down to 11.4%). It is also noted that the SCE rate remains

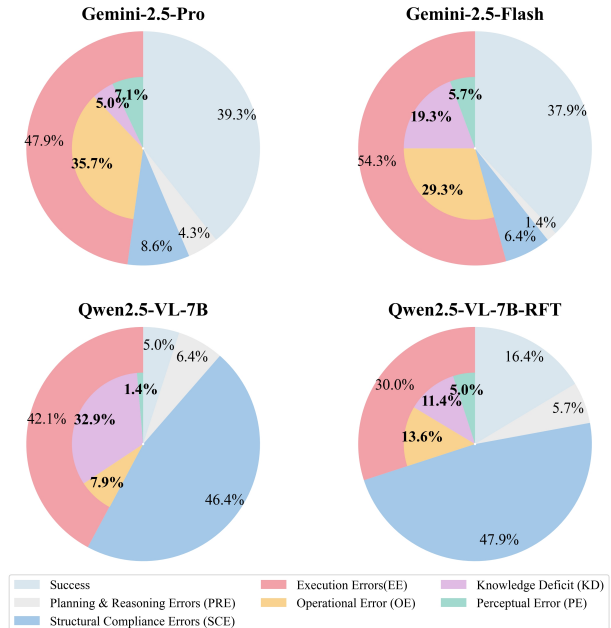


Figure 2: A comparative breakdown of failure modes for four vision-language models. The chart categorizes errors into three primary types: Planning & Reasoning Errors (PRE), Structural Compliance Errors (SCE), and Execution Errors (EE). The Execution Errors category is further subdivided into Operational Errors (OE), Knowledge Deficits (KD), and Perceptual Errors (PE).

at a relatively high level of 47.9%. This indicates that while our fine-tuning method effectively imparts domain knowledge to improve execution, it has not yet fully resolved the inherent challenges in structural compliance found in certain smaller models.

## 6 Conclusion and Discussion

To address the critical challenges in evaluating GUI agents, we introduce NaturalGAIA, a novel benchmark based on “Causal Pathways”, a hierarchical LightManus architecture, and a high-quality trajectory dataset featuring diverse and self-correcting behaviors. The experiments demonstrate that even state-of-the-art models like Claude-sonnet-4 face formidable challenges on NaturalGAIA, revealing deficiencies in long-horizon planning. Meanwhile, although Trajectory-Reinforced Fine-Tuning (T-RFT) enhances the foundational performance of smaller models (e.g., Qwen2.5-VL-7B), their capability ceiling in complex tasks remains constrained: while fine-tuning supplements some world knowledge, it struggles to fundamentally improve their operational precision and perceptual capabilities, and has not yet fully addressed the underlying challenge in structural compliance. This set of limitations highlights the critical gap between domain-specific skills and generalizable reasoning abilities.

While NaturalGAIA provides a robust standard, it does not fully capture the dynamic nature of real-world interfaces.

Future research can proceed in three directions: (1) developing agents with enhanced structural and logical reasoning abilities to overcome their innate bottlenecks; (2) creating dynamic benchmarks capable of auto-generating novel “Causal Pathways” to mitigate the risk of data contamination; (3) exploring advanced learning algorithms that can efficiently learn from self-correcting behaviors to build more resilient agents.

## References

Bai, J.; Bai, S.; Yang, S.; Wang, S.; Tan, S.; Wang, P.; Lin, J.; Zhou, C.; and Zhou, J. 2023. Qwen-VL: A Versatile Vision-Language Model for Understanding, Localization, Text Reading, and Beyond. arXiv:2308.12966.

Chai, Y.; Li, H.; Zhang, J.; Liu, L.; Liu, G.; Wang, G.; Ren, S.; Huang, S.; and Li, H. 2025. A3: Android Agent Arena for Mobile GUI Agents. arXiv:2501.01149.

Cheng, K.; Sun, Q.; Chu, Y.; Xu, F.; Li, Y.; Zhang, J.; and Wu, Z. 2024. SeeClick: Harnessing GUI Grounding for Advanced Visual GUI Agents. arXiv:2401.10935.

Chezelles, T. L. S. D.; Gasse, M.; Drouin, A.; Caccia, M.; Boisvert, L.; Thakkar, M.; Marty, T.; Assouel, R.; Shayegan, S. O.; Jang, L. K.; Lù, X. H.; Yoran, O.; Kong, D.; Xu, F. F.; Reddy, S.; Cappart, Q.; Neubig, G.; Salakhutdinov, R.; Chappados, N.; and Lacoste, A. 2025. The BrowserGym Ecosystem for Web Agent Research. arXiv:2412.05467.

DeepSeek-AI; et al. 2025. DeepSeek-R1: Incentivizing Reasoning Capability in LLMs via Reinforcement Learning. arXiv:2501.12948.

Deng, X.; Gu, Y.; Zheng, B.; Chen, S.; Stevens, S.; Wang, B.; Sun, H.; and Su, Y. 2023. Mind2Web: Towards a Generalist Agent for the Web. arXiv:2306.06070.

Durante, Z.; Huang, Q.; Wake, N.; Gong, R.; Park, J. S.; Sarkar, B.; Taori, R.; Noda, Y.; Terzopoulos, D.; Choi, Y.; Ikeuchi, K.; Vo, H.; Fei-Fei, L.; and Gao, J. 2024. Agent AI: Surveying the Horizons of Multimodal Interaction. arXiv:2401.03568.

Garg, D.; VanWeelden, S.; Caples, D.; Draguns, A.; Ravi, N.; Putta, P.; Garg, N.; Abraham, T.; Lara, M.; Lopez, F.; Liu, J.; Gundawar, A.; Hebbar, P.; Joo, Y.; Gu, J.; London, C.; de Witt, C. S.; and Motwani, S. 2025. REAL: Benchmarking Autonomous Agents on Deterministic Simulations of Real Websites. arXiv:2504.11543.

Gou, B.; Wang, R.; Zheng, B.; Xie, Y.; Chang, C.; Shu, Y.; Sun, H.; and Su, Y. 2025. Navigating the Digital World as Humans Do: Universal Visual Grounding for GUI Agents. arXiv:2410.05243.

He, H.; Yao, W.; Ma, K.; Yu, W.; Dai, Y.; Zhang, H.; Lan, Z.; and Yu, D. 2024. WebVoyager: Building an End-to-End Web Agent with Large Multimodal Models. arXiv:2401.13919.

He, Y.; Jin, J.; and Liu, P. 2025. Efficient Agent Training for Computer Use. arXiv:2505.13909.

Hong, W.; Wang, W.; Lv, Q.; Xu, J.; Yu, W.; Ji, J.; Wang, Y.; Wang, Z.; Zhang, Y.; Li, J.; Xu, B.; Dong, Y.; Ding, M.; and Tang, J. 2024. CogAgent: A Visual Language Model for GUI Agents. arXiv:2312.08914.

Huang, Z.; Zou, H.; Li, X.; Liu, Y.; Zheng, Y.; Chern, E.; Xia, S.; Qin, Y.; Yuan, W.; and Liu, P. 2024. O1 Replication Journey – Part 2: Surpassing O1-preview through Simple Distillation, Big Progress or Bitter Lesson? arXiv:2411.16489.

Jiang, W.; Zhuang, Y.; Song, C.; Yang, X.; and Zhang, C. 2025. AppAgentX: Evolving GUI Agents as Proficient Smartphone Users. arXiv:2503.02268.

Koh, J. Y.; Lo, R.; Jang, L.; Duvvur, V.; Lim, M.; Huang, P.-Y.; Neubig, G.; Zhou, S.; Salakhutdinov, R.; and Fried, D. 2024a. VisualWebArena: Evaluating Multimodal Agents on Realistic Visual Web Tasks. In Ku, L.-W.; Martins, A.; and Srikanth, V., eds., *Proceedings of the 62nd Annual Meeting of the Association for Computational Linguistics (Volume 1: Long Papers)*, 881–905. Bangkok, Thailand: Association for Computational Linguistics.

Koh, J. Y.; Lo, R.; Jang, L.; Duvvur, V.; Lim, M. C.; Huang, P.-Y.; Neubig, G.; Zhou, S.; Salakhutdinov, R.; and Fried, D. 2024b. VisualWebArena: Evaluating Multimodal Agents on Realistic Visual Web Tasks. arXiv:2401.13649.

Li, K.; Meng, Z.; Lin, H.; Luo, Z.; Tian, Y.; Ma, J.; Huang, Z.; and Chua, T.-S. 2025a. ScreenSpot-Pro: GUI Grounding for Professional High-Resolution Computer Use. arXiv:2504.07981.

Li, Z.; You, K.; Zhang, H.; Feng, D.; Agrawal, H.; Li, X.; Moorthy, M. P. S.; Nichols, J.; Yang, Y.; and Gan, Z. 2025b. Ferret-UI 2: Mastering Universal User Interface Understanding Across Platforms. arXiv:2410.18967.

Liu, G.; Zhao, P.; Liu, L.; Guo, Y.; Xiao, H.; Lin, W.; Chai, Y.; Han, Y.; Ren, S.; Wang, H.; Liang, X.; Wang, W.; Wu, T.; Li, L.; Wang, H.; Xiong, G.; Liu, Y.; and Li, H. 2025a. LLM-Powered GUI Agents in Phone Automation: Surveying Progress and Prospects. arXiv:2504.19838.

Liu, H.; Zhang, X.; Xu, H.; Wanyan, Y.; Wang, J.; Yan, M.; Zhang, J.; Yuan, C.; Xu, C.; Hu, W.; and Huang, F. 2025b. PC-Agent: A Hierarchical Multi-Agent Collaboration Framework for Complex Task Automation on PC. arXiv:2502.14282.

Liu, X.; Yu, H.; Zhang, H.; Xu, Y.; Lei, X.; Lai, H.; Gu, Y.; Ding, H.; Men, K.; Yang, K.; Zhang, S.; Deng, X.; Zeng, A.; Du, Z.; Zhang, C.; Shen, S.; Zhang, T.; Su, Y.; Sun, H.; Huang, M.; Dong, Y.; and Tang, J. 2023. AgentBench: Evaluating LLMs as Agents. arXiv:2308.03688.

Mialon, G.; Fourrier, C.; Swift, C.; Wolf, T.; LeCun, Y.; and Scialom, T. 2023. GAIA: a benchmark for General AI Assistants. arXiv:2311.12983.

Muennighoff, N.; Yang, Z.; Shi, W.; Li, X. L.; Fei-Fei, L.; Hajishirzi, H.; Zettlemoyer, L.; Liang, P.; Candès, E.; and Hashimoto, T. 2025. s1: Simple test-time scaling. arXiv:2501.19393.

OpenAI; et al. 2024a. GPT-4 Technical Report. arXiv:2303.08774.

OpenAI; et al. 2024b. OpenAI o1 System Card. arXiv:2412.16720.

Qiu, J.; Qi, X.; Zhang, T.; Juan, X.; Guo, J.; Lu, Y.; Wang, Y.; Yao, Z.; Ren, Q.; Jiang, X.; Zhou, X.; Liu, D.; Yang,

L.; Wu, Y.; Huang, K.; Liu, S.; Wang, H.; and Wang, M. 2025. Alita: Generalist Agent Enabling Scalable Agentic Reasoning with Minimal Predefinition and Maximal Self-Evolution. *arXiv:2505.20286*.

Qwen; et al. 2025. Qwen2.5 Technical Report. *arXiv:2412.15115*.

Rasheed, H.; Maaz, M.; Mullappilly, S. S.; Shaker, A.; Khan, S.; Cholakkal, H.; Anwer, R. M.; Xing, E.; Yang, M.-H.; and Khan, F. S. 2024. GLaMM: Pixel Grounding Large Multi-modal Model. *arXiv:2311.03356*.

Rawles, C.; Clinckemaillie, S.; Chang, Y.; Waltz, J.; Lau, G.; Fair, M.; Li, A.; Bishop, W.; Li, W.; Campbell-Ajala, F.; Toyama, D.; Berry, R.; Tyamagundlu, D.; Lillicrap, T.; and Riva, O. 2024. AndroidWorld: A Dynamic Benchmarking Environment for Autonomous Agents. *arXiv:2405.14573*.

Shinn, N.; Cassano, F.; Berman, E.; Gopinath, A.; Narasimhan, K.; and Yao, S. 2023. Reflexion: Language Agents with Verbal Reinforcement Learning. *arXiv:2303.11366*.

Tang, F.; Xu, H.; Zhang, H.; Chen, S.; Wu, X.; Shen, Y.; Zhang, W.; Hou, G.; Tan, Z.; Yan, Y.; Song, K.; Shao, J.; Lu, W.; Xiao, J.; and Zhuang, Y. 2025. A Survey on (M)LLM-Based GUI Agents. *arXiv:2504.13865*.

Wang, G.; Xie, Y.; Jiang, Y.; Mandlekar, A.; Xiao, C.; Zhu, Y.; Fan, L.; and Anandkumar, A. 2023. Voyager: An Open-Ended Embodied Agent with Large Language Models. *arXiv:2305.16291*.

Wang, J.; Xu, H.; Jia, H.; Zhang, X.; Yan, M.; Shen, W.; Zhang, J.; Huang, F.; and Sang, J. 2024. Mobile-Agent-v2: Mobile Device Operation Assistant with Effective Navigation via Multi-Agent Collaboration. *arXiv:2406.01014*.

Wang, Z.; Xu, H.; Wang, J.; Zhang, X.; Yan, M.; Zhang, J.; Huang, F.; and Ji, H. 2025. Mobile-Agent-E: Self-Evolving Mobile Assistant for Complex Tasks. *arXiv preprint arXiv:2501.11733*.

Xu, Y.; Liu, X.; Sun, X.; Cheng, S.; Yu, H.; Lai, H.; Zhang, S.; Zhang, D.; Tang, J.; and Dong, Y. 2024. AndroidLab: Training and Systematic Benchmarking of Android Autonomous Agents. *arXiv:2410.24024*.

Yang, S.; Nachum, O.; Du, Y.; Wei, J.; Abbeel, P.; and Schuurmans, D. 2023. Foundation Models for Decision Making: Problems, Methods, and Opportunities. *arXiv:2303.04129*.

Ye, S.; Shi, H.; Shih, D.; Yun, H.; Roosta, T.; and Shu, T. 2025a. RealWebAssist: A Benchmark for Long-Horizon Web Assistance with Real-World Users. *arXiv:2504.10445*.

Ye, Y.; Huang, Z.; Xiao, Y.; Chern, E.; Xia, S.; and Liu, P. 2025b. LIMO: Less is More for Reasoning. *arXiv:2502.03387*.

Zhang, C.; Huang, H.; Ni, C.; Mu, J.; Qin, S.; He, S.; Wang, L.; Yang, F.; Zhao, P.; Du, C.; Li, L.; Kang, Y.; Jiang, Z.; Zheng, S.; Wang, R.; Qian, J.; Ma, M.; Lou, J.-G.; Lin, Q.; Rajmohan, S.; and Zhang, D. 2025. UFO2: The Desktop AgentOS. *arXiv:2504.14603*.

Zhang, W.; Tang, K.; Wu, H.; Wang, M.; Shen, Y.; Hou, G.; Tan, Z.; Li, P.; Zhuang, Y.; and Lu, W. 2024. Agent-Pro: Learning to Evolve via Policy-Level Reflection and Optimization. *arXiv:2402.17574*.

Zhang, X.; Lu, Y.; Wang, W.; Yan, A.; Yan, J.; Qin, L.; Wang, H.; Yan, X.; Wang, W. Y.; and Petzold, L. R. 2023. GPT-4V(ision) as a Generalist Evaluator for Vision-Language Tasks. *arXiv:2311.01361*.

Zhou, S.; Xu, F. F.; Zhu, H.; Zhou, X.; Lo, R.; Sridhar, A.; Cheng, X.; Bisk, Y.; Fried, D.; Alon, U.; et al. 2023. WebArena: A Realistic Web Environment for Building Autonomous Agents. *arXiv preprint arXiv:2307.13854*.